Efficient synthesis of a new electroactive polymer of Co(II) porphine by in-situ replacement of Mg(II) inside Mg(II) polyporphine film

Sébastien D Rolle, Dmitry V Konev, Charles H. Devillers, Ksenia V Lizgina, Dominique Lucas, Christine Stern, Frédéric Herbst, Olivier Heintz, Mikhail A Vorotyntsev

Efficient synthesis of a new electroactive polymer of Co(II) porphine by *in-situ* replacement of Mg(II) inside Mg(II) polyporphine film

Sébastien D. Rolle[a], Dmitry V. Konev[b,e]*, Charles H. Devillers[a]*, Ksenia V. Lizgina[c], Dominique Lucas[a]*, Christine Stern[a], Frédéric Herbst[d], Olivier Heintz[d], Mikhail A. Vorotyntsev[a,b,c,e]*

[a] ICMUB UMR6302, CNRS, Univ. Bourgogne Franche-Comté, F-21000 Dijon, France

[b] Institute for Problems of Chemical Physics of the Russian Academy of Sciences, Chernogolovka, Russia

[c] M.V. Lomonosov Moscow State University, Moscow, Russia

[d] Laboratoire Interdisciplinaire Carnot de Bourgogne, UMR CNRS 5209, Université de Bourgogne Franche-Comté, 21078 Dijon, France

[e] D. I. Mendeleev University of Chemical Technology of Russia, Moscow, Russia

Abstract

This paper presents an easy, efficient and reproducible way to obtain cobalt polyporphine films. A fast three step process (less than one hour) based on electrosynthesis of magnesium polyporphine of type I followed by a demetallation in acid medium and then cobalt insertion inside the porphine units allowed us to obtain an interesting material with a high density of active cobalt(II) centers. Kinetics studies were conducted to determine the best conditions for the demetallation and remetallation steps. Moreover, IR-ATR and UV-visible measurements attested that the initial molecular structure of the porphine units was kept during the three step process. Qualitative composition of polyporphine films has been confirmed via XPS and EDX methods. In situ specific conductivity of these polyporphine polymers of type I has been determined as a function of the imposed potential, i.e. of the oxidation degree.

Keywords: electroactive materials, electropolymerization, ion-exchange, cobalt porphine, non-substituted porphyrins, metalloporphines.

1. Introduction

Porphyrin-based thin films are currently used in various fields and for many applications because of their interesting physico-chemical properties [1]. Indeed, these materials operate in different devices for nonlinear optical and optical limiting devices [2], photoluminescent biosensors [3], electrochemical or spectrometric sensors [4-12], molecular electronic junctions [13-14] and electrocatalytic systems [15-16]. Previous studies of our group have shown that the electrochemical oxidation at low potential of the fully unsubstituted porphyrin, *i.e*. magnesium(II) porphine (**MgP**) led to the formation of an electroactive magnesium(II) polyporphine films on the electrode surface *via* C_{meso}-C_{meso} coupling [17-22]. This polymer was named type I magnesium polyporphine **pMgP-I**.

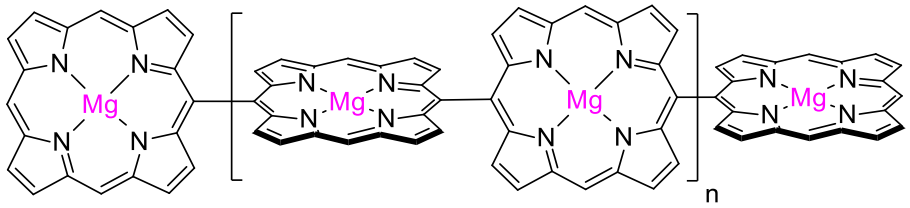

Fig. 1 Plausible structure of Magnesium(II) polyporphine of type I.

Recently, we described the synthesis of zinc(II) polyporphine by ion-exchange of Mg(II) by Zn(II) cations inside the Mg(II) polyporphine film [21]. This three step synthesis starts with the formation of the **pMgP-I** material according to known procedures [18-20,22]. Then, demetallation of the polymer is achieved by addition of trifluoroacetic acid (TFA). Finally, Zn(II) cations are chemically inserted in the resulting free-base polyporphine (**pH_2P-I**) material leading to the zinc(II) polyporphine of type I (**pZnP-I**).

Numerous studies have reported that Co(II) porphyrins are useable as sensing molecules for the detection of many different substances such as sulphites or volatile organic compounds [8-9,23-26]. These cobalt complexes have also been exploited as electrocatalysts for fuel or solar cells [27-30]. However, none of this previous works was using a polyporphine material. Indeed, Co(II) porphyrins are often dispersed in a electropolymerizable matrix or included in a copolymer. Besides, some authors made profit of electropolymerizable substituents grafted on the periphery of the porphyrin macrocycle to generate new polymeric films. Consequently, the density of metallic active centers which are located in the porphyrin macrocycle is reduced and this feature could limit the sensitivity and/or the efficiency of the material.

Thus, this paper describes the synthesis of an unprecedented Co(II) polyporphine of type I (**pCoP-I**) following a similar but improved process than the one previously described by us for the synthesis of **pZnP-I** [21]. This new material should logically exhibit the highest density of metallic centers ever available for a porphyrin-based material. **pCoP-I** is synthesized in three steps: 1) synthesis of **pMgP-I**, 2) demetallation and 3) insertion of cobalt(II) inside the porphine units. In particular, steps 2) and 3) have been optimized. Concerning the demetallation step, two different acids have been tested. Regarding the third cobalt(II) remetallation step, two chemical cobalt(II) containing precursors have been compared. Kinetics of the two last steps has also been studied. Moreover, the repeatability and reproducibility of the whole process have been demonstrated as well as the conservation of the initial polymer molecular structure. The characterization of these different polymers deposited on GC, Pt or ITO has been carried out by electrochemical (voltammetry, in situ conductivity) and spectroscopic (UV-visible, IR-ATR, XPS, SEM-EDX) measurements.

2. Experimental

The MgP monomer was synthesized following Lindsey's procedure [31] and ultimately purified according to Devillers *et al* [32].

Acetonitrile (AN) was HPLC grade (Prolabo) and was distilled over CaH_2 under Ar. Tetra-*n*-butylammoniumhexafluorophosphate ($TBAPF_6$) was synthesized by mixing stoichiometric amounts of tetra-*n*-butylammonium hydroxide (Alfa-Aesar, 40% w/w aq soln) and hexafluorophosphoric acid (Alfa-Aesar, *ca*. 60% w/w aq soln). After filtration, the salt was recrystallized three times in ethanol and dried at 110 °C during at least 2 days.

Electrochemical measurements (film deposition and its characterization in the monomer-free solution) were performed in AN under an Ar atmosphere in a three-electrode glass cell. Working electrodes (WE) were Pt and glassy carbon (GC) disks with surface areas of about 0.01 (Pt), 0.03 (Pt) and 0.07 (GC) cm² or ITO-layer covered glass plate. Pt wire was used as counter electrode (CE). Either saturated aqueous calomel (SCE) or Ag/0.01 M $AgNO_3$ + 0.1 M $TBAPF_6$ in AN electrodes were used as reference electrodes (RE). The RE was separated from the WE compartment by a double frit comprising an intermediate background solution (0.1 M $TBAPF_6$ + AN). All the potentials in this manuscript are indicated vs. SCE. In these conditions, the $E_{1/2}$ for the Fc^+/Fc couple is 0.40 V vs. SCE. All the electrochemical studies were realized using Autolab PGSTAT 302N potentiostat and Elins PI50RPO3.

All potentials in this paper are given *versus* SCE. All potentiodynamic experiments (CV) (redox response of films) were performed at the scan rate of 100 mV/s unless otherwise noted.

The initial polymeric films of magnesium(II) porphine were deposited by potentiostatic polymerization at 0.65 V in a polymerization bath containing 0.5 mM of MgP and 1.5 mM of 2,6-lutidine in $TBAPF_6$ 0.1 M in AN (to improve polymerization efficacy [22]). The polymerization was automatically stopped when the deposition charge reached 10 mC/cm².

To remove Mg(II) in the polymers, electrodes coated with pMgP-I were carefully rinsed with AN and placed during 5 to 60 min (see below) in a 0.2 M acid solution in AN under Ar atmosphere at room temperature. Two different acids were tested: trifluoroacetic acid (TFA) and hydrochlorhydric acid (HCl). Then, the films were rinsed with a 2.5% NH_3 solution in AN to recover the free base form (pH_2P-I, see below) and they were finally rinsed with AN for further studies.

To insert Co(II) in the porphine macrocycle, pH_2P-I modified electrodes were dipped in a cobalt(II) acetate saturated solution in dimethylformamide (DMF) and warmed at 110 °C or 80 °C during 5 to 60 min, under argon (see below). DMF (HPLC Grade) and $Co(OAc)_2.4H_2O$ were purchased from Carlo Erba. These pCoP-I films were then carefully rinsed with distilled H_2O and AN before characterization.

IR film characterization was performed with films deposited on Pt disks (0.03 cm²). IR Spectra were obtained by ATR method with a Bruker LUMOS spectrophotometer. UV-vis absorption measurements were performed on modified ITO plates with a VARIAN UV-visible spectrophotometer Cary 50 scan.

Samples for XPS measurements were prepared analogously. They were performed with the use of SIA100 device (Cameca Riber apparatus) with non-monochromatized Al Kα source (1486.6 eV). SEM imaging accompanied by EDX analysis was performed with scanning electronic microscope JEOL JSM6400F equipped by Oxford Instruments EDS analyzer.

3. Results and discussion

Scheme 1 shows the successive steps leading to the target Co(II) polyporphine film (pCoP-I). The optimized experimental conditions for demetallation and remetallation steps were defined according to the results of kinetics studies (see part 3.2.).

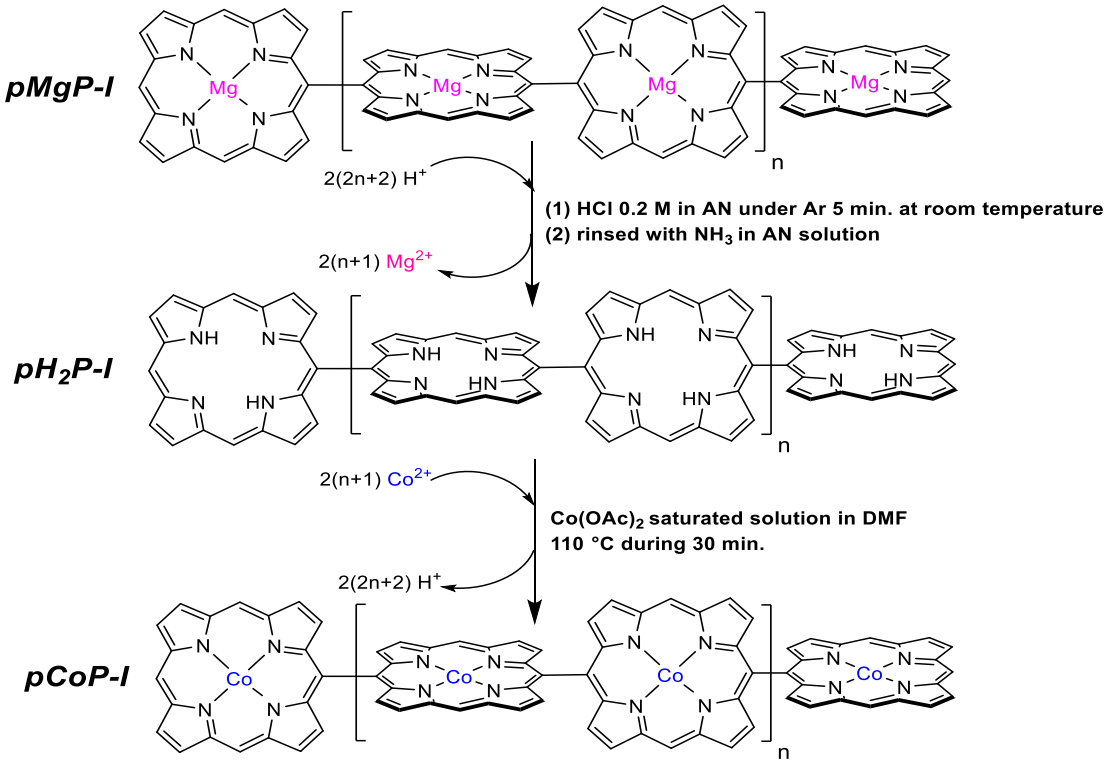

Scheme 1 : Synthesis of **pCoP-I** starting from **pMgP-I.**

As a previous step, electropolymerization of pMgP-I film, is conducted according conditions established in our precedent works [18-20,22].

Thereafter, the Mg(II) cations are removed from the macrocycle centers with an acidic treatment, either with HCl or TFA (see part 3.2). However, especially with HCl, the electrochemical response of polyporphine films is accompanied by an large additional redox signal at E_{pc} = -0.35 V which probably corresponds to the reduction of the dicationic and tetraprotonated form (pH_4P^{2+}-I) of the porphine unit which is formed in these strongly acidic conditions [21,33-34]. To remove these protons, the film is rinsed with a NH_3 solution to obtain the neutral free-base porphine polymer, pH_2P-I.

Initially inspired by previous works [35-37], the cobalt(II) remetallation conditions of the free-base polyporphine film were further optimized (see 3.2.).

Globally, pCoP-I is synthesized in three steps from MgP monomer keeping the same molecular structure as pMgP-I. The whole three-step process lasts less than 2 h including the intermediate electrochemical analyses by which, at each step, the reaction progress is controlled.

3.1. Electrochemical response of the different polymers and their conductivity

Fig. 2 shows the evolution of the cyclic voltammograms of the polyporphine film at each step of its transformation (pMgP-I $\rightarrow$ pH_2P-I $\rightarrow$ PCoP-I). All the different peaks are identified and their characteristics are gathered in Table 1.

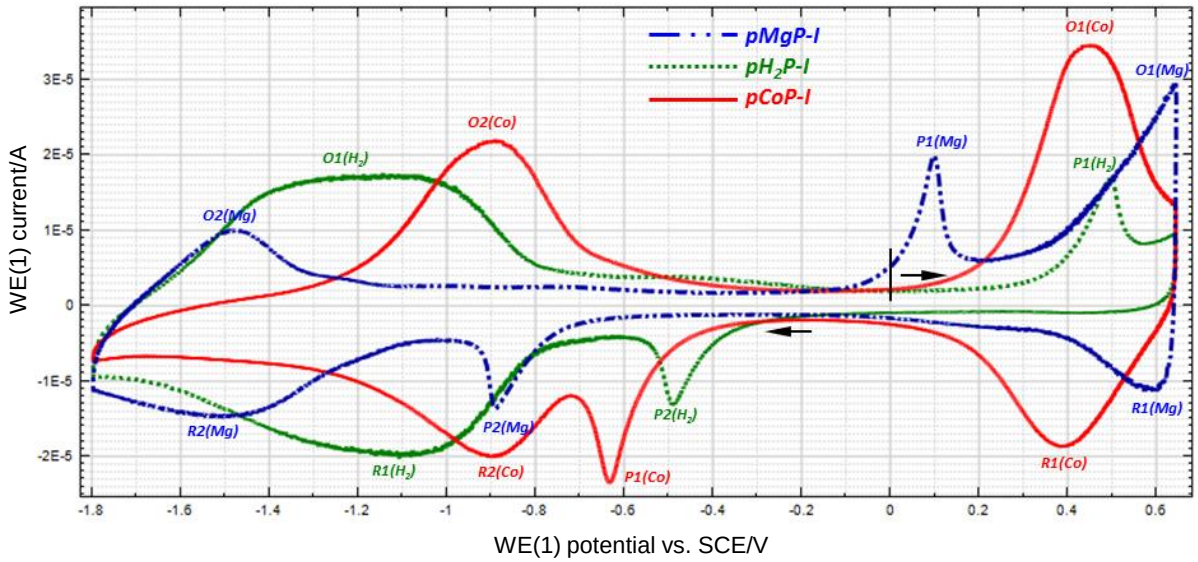

Fig. 2. Cyclic voltammograms (5th cycle, between -1.8 and 0.645 V) of **pMgP-I** (blue dashed curve), **pH$_2$P-I** (green dotted line, resulting from the demetallation of **pMgP-I** with 0.2 M HCl, followed by NH_3 solution rinsing) and **pCoP-I** (red solid line, resulting from the metallation with a saturated $Co(OAc)_2$ solution in DMF at 110 °C) films deposited on GC disk (AN 0.1 M $TBAPF_6$, v = 0.1 V s^{-1}).

Table 1. Relevant parameters for the peaks displayed on Fig. 2 (films deposited on GC disk, AN 0.1 M $TBAPF_6$, v = 0.1 V s^{-1}).

pMgP-I	Characteristics signal	**O1(Mg)**	**O2(Mg)**	**R1(Mg)**	**R2(Mg)**	**P1(Mg)**	**P2(Mg)**
	Peak potential (V)	0,65	-1,48	0,59	-1,50	0,10	-0,89
	Charge (µC)	5,8	3,2	-2,5	-7,4	3,6	-2,7
	Peak intensity (µA)	29,8	10,1	-11,1	-14,7	19,9	-13,5
	Intensity RSD (%)[a]	2,8			3,8		
pH$_2$P-I	Characteristics signal	**O1(H$_2$)**		**R1(H$_2$)**		**P1(H$_2$)**	**P2(H$_2$)**
	Peak potential (V)	-1,20 (large)		-1,10 (large)		0,50	-0,49
	Charge (µC)	11,5		-14,5		2,5	-2,2
	Peak intensity (µA)	17,2		-19,6		16,9	-13,2
	Intensity RSD (%)[a]	3,0		0,9			
pCoP-I	Characteristics signal	**O1(Co)**	**O2(Co)**	**R1(Co)**	**R2(Co)**	**P1(Co)**	
	Peak potential (V)	0,45	-0,90	0,39	-0,90	-0,63	
	Charge (µC)	10,2	6,9	-5,6	-7,3	-4,0	
	Peak intensity (µA)	34,4	21,7	-18,6	-19,8	-23,4	
	Intensity RSD (%)[a]	6,2			1,6		

[a] calculated from three different modified electrodes.

The voltammogram of pMgP-I (blue dashed curve, Fig. 2) exhibits two reversible systems at 0.645 V (O1(Mg)/R1(Mg)) and -1.50 V (R2(Mg)/(O2(Mg)) which correspond, respectively, to the first oxidation and reduction of the Mg(II) porphine units into their cation and anion radicals [18-20,22].

Only one large reversible system located at around -1.2 V (O1(H_2)/R1(H_2)) is observed on the pH$_2$P-I voltammogram (green dotted curve, Fig. 2). According to previous works [21] and free-base porphyrin electrochemical studies in solution [33,38-40], this large peak corresponds to the superimposition of two consecutive and merged reductions of the free-base porphine units. Moreover, the full disappearance of the O1(Mg)/R1(Mg) system suggests that nearly all Mg(II) cations were removed from the porphine units in the demetallation process.

The voltammogram of pCoP-I exhibits two reversible systems at *ca*. 0.4 V (O1(Co)/R1(Co)) and -0.90 V (O2(Co)/R2(Co)). O1(Co)/R1(Co) peaks are attributed to the Co(II)/Co(III) redox couple [29-30,41-43] whereas the second system O2(Co)/R2(Co) around -0.9 V is ascribed to the reversible Co(I)/Co(II) redox couple, being similar to the typical response of cobalt porphyrins in solution.[42] These

characteristic signals seems to confirm that the Co(II) cations are truly complexed by the porphine macrocycles and not scattered in the film apart from the porphine structure.

As previously described [18-20,22], pMgP-I polymer shows a large interval of non-electroactivity between *ca*. –0.7 V and -0.1 V. The limits of this potential interval are marked by two prepeaks, P1(Mg) and P2(Mg). The non-electroactivity domain is also observed for pH_2P-I but between *ca*. -0.3 V and 0.3 V. Prepeaks P1(H_2) and P2(H_2) are also observed, but at more positive potentials than for pMgP-I, *i.e*. at 0.50 V and -0.49 V. In a similar way, pCoP-I film shows a non-electroactive interval between *ca*. -0.4 V and 0.1 V. Besides, only one prepeak, P1(Co) is seen at -0.63 V. The expected second oxidation prepeak is apparently masked by the O1(Co) peak. According to S. Cosnier *et al*. [44-46], J. Jiping *et al*. [47], S. Gottesfeld *et al*. [48] and M. A. Vorotyntsev *et al* [49], these prepeaks are in relation with the polymer charge/discharge process. Indeed, when the polymer is charged during a forward voltammetric cycle, the corresponding discharge is not fast enough to be completed before reaching again the non-electroactivity interval. Thus, the residual charge is eliminated later during the backward cycle, when the polymer becomes conductive again. This hypothesis seems to be confirmed by the charge calculation. Thus, the area under O1(Mg) peak (5.75 µC) is very similar to the one corresponding to the charge measured for the sum of R1(Mg) and P2(Mg) peak areas (2.5 + 2.75 = 5.25 µC). Furthermore, similar observations can be made for R2(Mg)/(O2(Mg)+P1(Mg)) and R1(H_2)/O1(H_2)/P1(H_2) couples (7.40 vs. (3.22 + 3.59) µC, and 14.45 vs. (11.54 + 2.48) µC, respectively). However, in the particular case of pCoP-I film, it is impossible to perform this calculation due to the merging of the oxidation prepeak (P1(Co)) with O1(Co) peak. The remanence of non-electroactive intervals and prepeaks for pMgP-I, pH_2P-I and pCoP-I materials is in accordance with the molecular structure of the initial pMgP-I polymer being retained during the demetallation/remetallation sequence.

In order to demonstrate the process repeatability [50-51], three different polymers were synthetized on a GC disk electrode following the procedure described in scheme 1. All the experiments were done during the same day by the same operator according to ISO definition. The initial polymerization cell, the demetallation and remetallation solutions and the blank solution were identical for all polymers. The repeatability was evaluated using the Relative Standard Deviation (RSD) calculation. A RSD value below 10% means that the ion-exchange process is repeatable. Results are presented in Table 1 at each step of the polymer transformation. Charge controlled polymerization of magnesium polyporphine polymer allows obtaining polymers with repeatable electrochemical properties. Thus, the calculated RSDs for pMgP-I peak intensities are less than 5% which demonstrates the fidelity of this 1st step. Moreover, after demetallation, variation of the free-base polyporphine peak intensities is also very low, less than 3%. So, the demetallation step using HCl 0.2 M in AN during 5 min at room temperature does not damage the process fidelity. Finally, repeatable electrochemical features were also obtained after the remetallation step. The RSD remains very low, not exceeding 10% for all the peak intensities in spite of the high temperature and duration of the process (110 °C, 30 min.), as well as the good solubilizing ability of DMF, which may be potentially damaging for the polymer.

Analogous transformation of polyporphine films has been achieved for the Pt electrode surface with the use of the same procedure (Fig. 3). Parameters of oxidation and reduction waves for this electrode were similar to those on GC (Fig. 2).

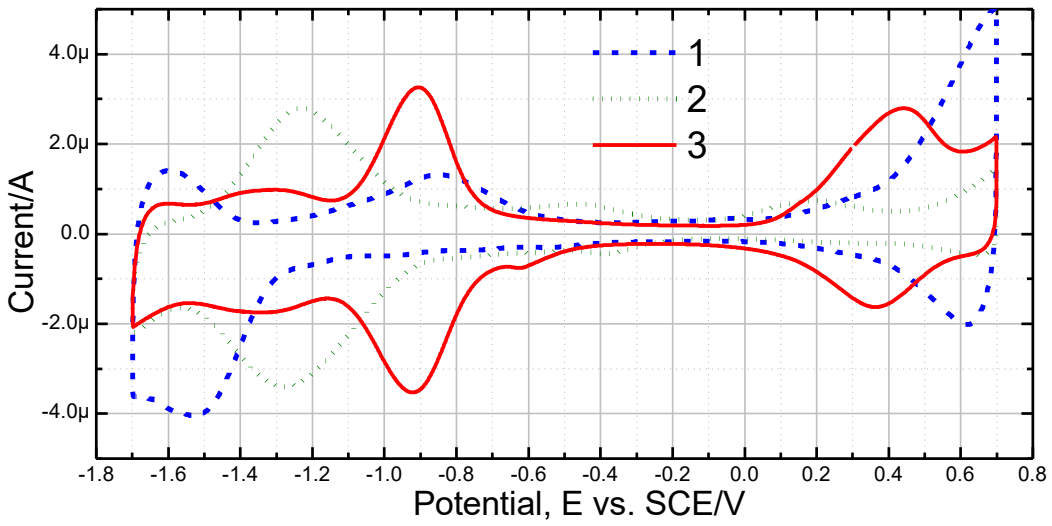

Fig. 3. CV plots for various polyporphine films, pMP-I, on the Pt electrode surface in contact with background solution, 0.1 M $TBAPF_6$ in AN, v = 0.1 V s^{-1}. Curve 1 corresponds to the Mg polyporphine deposited with the use of the procedure [22] with addition of the proton acceptor, lutidine, into the polymerization bath (deposition charge: 9.5 mC/cm^2). Free-base polyporphine of type I, pH_2P-I (curve 2), was obtained from pMgP-I by 10-minute treatment by TFA acid in AN. Co(II) polyporphine of type I, pCoP-I (curve 3) was synthesized by metallation of pH_2P-I with DMF solution of $Co(OAc)_2 \cdot 4H_2O$ (10 mg/ml) for 60 min at 75-85°C.

In summary, the RSD of the peak intensities does not significantly increase during the demetallation and remetallation steps, as expected if the polyporphine film is not degraded by the diverse treatments applied in view of its transformation.

One of the principal characteristics of electroactive films is their specific conductivity as a function of the imposed potential, i.e. of the oxidation degree of the film. For its determination for polyporphine films on electrode surface we have applied a recently proposed method [52] based on measurement of the "high-frequency resistance" composed of the disk working electrode (its diameter being small compared to the distances between its surface and other electrodes of the cell) coated by the film which is in contact with background electrolyte solution (0.1 M $TBAPF_6$ in AN in the present study). The system is perturbed by a potential step (amplitude: δE = 100 mV) resulting in instantaneous generation of the "primary distributions" of the current density and potential inside the film and the solution layer near the electrode surface. Chronoamperogram, i.e. the current variation within a short-time interval after the potential step was registered with a high temporal resolution (every 2 microseconds). Extrapolation of this short-time plot (within the 20 to 30 μs interval) in the semi-logarithmic coordinates (log I(t), t) to the potential-step moment gave the value of the instantaneous current, I^o, which was re-calculated in terms of the overall resistance of the film+solution system, $R_{tot} = \delta E / I^o$. This resistance value was used to determine the film resistance, R_f, as well as the specific conductivity of the film, κ, with the use of the relation: $\kappa = L / (S R_f)$ [52] (for the value of L, see part 3.6. SEM-EDX). This procedure was performed for a set of the electrode potential values, thus providing the $\kappa(E)$ dependence for the film.

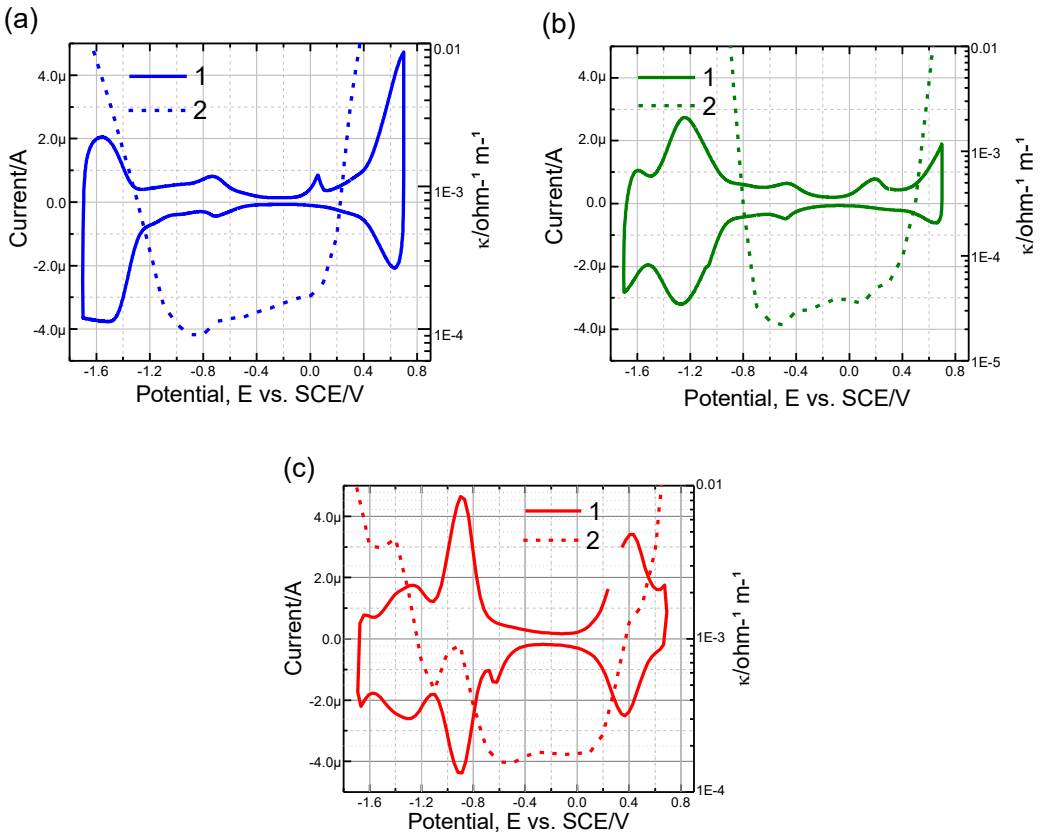

Fig. 4. Cyclic voltammograms (solid lines 1) and specific conductivity (dotted lines 2) of various polyporphine films of type I, pMP-I (M = Mg^{2+} in Fig 3a, M = $2H^{+}$ in Fig 3b, M = Co^{2+} in Fig 3c) deposited on the Pt disk electrode surface. CV measurements were performed in contact with 0.1 M $TBAPF_6$ + AN solution. *v* = 0.1 V s^{-1}).

For all studied polyporphines (pMgP-I, pH_2P-I and pCoP-I) the results of the CV and conductivity measurements (Fig. 4) confirm the correlation between these properties, in analogy with observations for most conjugated polymers. Within the potential ranges where the film possesses a high electroactivity the total resistance of the electrode/film system becomes close to that of the non-coated electrode. Since their values coincide with one another within the experimental dispersion of the data the specific conductivity under the conditions of the actual study (electrode surface, high-frequency solution resistance, film thickness) could only be measured with the use of this technique for its values below 0.01 S/cm.

The found dependences of the conductivity of the films, pMgP-I, pH_2P-I and pCoP-I, on their oxidation state show a similar shape for all these systems, in particular the levels of their conductivities and electroactivities are correlated. The lowest conductivity among them in the neutral state of the polymer is demonstrated by the metal-free polymer, pH_2P-I, while the minimal conductivities are close to one another for both metal-containing films. This difference may be tentatively attributed to the absence of axially coordinated solvent molecules in the former polymer, thus leading to a more compact structure of the film in its neutral state. On the contrary, the presence of coordinated solvent molecules in poly(metal porphine)s results in a more loose polymer structure, with expected incorporation of the background electrolyte components and their easier displacement by the electric field, i.e. corresponding to a higher conductivity in the neutral state of the polymer.

A slight distinction of the conductivity vs. potential dependence takes place for the cobalt polyporphine, pCoP-I (Fig. 4c). Namely, one can observe an upward deviation of the conductivity from the universal behavior for polyporphines within the potential range of the Co(I)/Co(II) and

Co(II)/Co(III) redox transitions. It implies the coexistence of two different electron-transport mechanisms within these potential intervals: both the charge propagation along the conjugated π-electron system of the polymer backbone and the hopping transport between neighboring redox centers, i.e. between Co ions inside the porphine monomer units having different oxidation degrees.

3.2. Kinetics studies

The magnesium(II) cations of pMgP-I were removed by immersion of the polymer in a 0.2 M TFA or HCl solution in AN. The kinetics of this demetallation step was followed on GC modified electrodes under Ar at room temperature by monitoring the pH_2P-I CV peak intensity $|i_{corr}|$ at -1.2 V ($|i_{corr}| = |i_t| - |i_0|$ with i_t = current intensity measured at −1.2 V and i_0 = initial current measured at −1.2 V before demetallation) as a function of time (Fig. 5). TFA and HCl have been chosen since these acids are commonly used for porphyrin demetallation.[21,53-56] After a given reaction time, the modified electrode was rinsed with a NH_3 solution, AN and then the CV response of the polyporphine film was recorded.

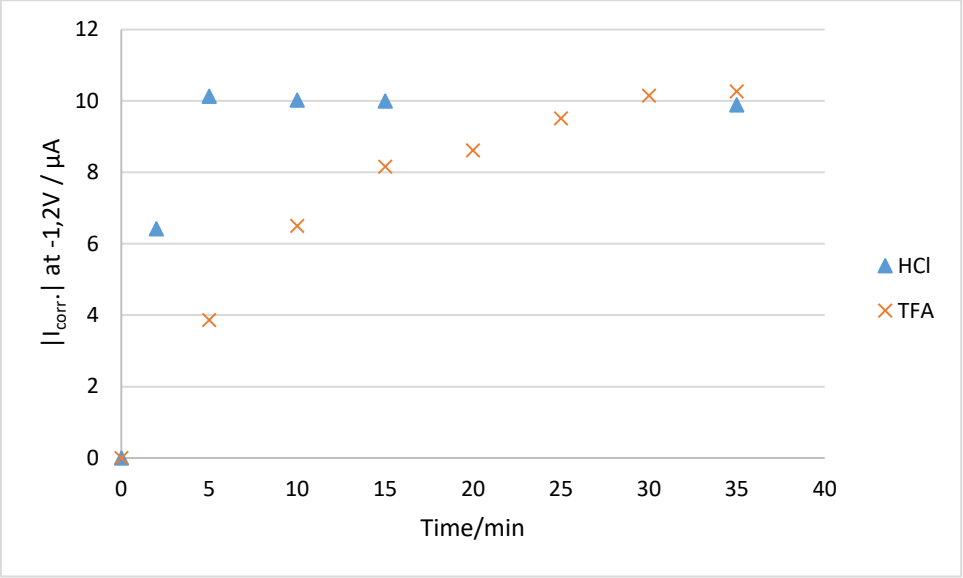

Fig. 5. Room temperature evolution of the CV peak intensity $|i_{corr}|$ measured at −1.2 V (characteristic of pH_2P-I material) as a function of time ($|i_{corr}| = |i_t| - |i_0|$ with i_t = current intensity measured at −1.2 V and i_0 = initial current measured at −1.2 V before demetallation (pMgP-I film)) and as a function of the used acid (TFA or HCl at 0.2 M in AN); WE: modified GC electrode.

As evidenced in Fig. 5, the reaction is much faster with HCl than with TFA. Indeed, with the former, $i_{corr.}$ reaches a plateau after 5 min. indicating a nearly complete conversion whereas 30 min. are necessary with TFA to attain the same level of $i_{corr.}$. This clear difference of efficiency between the two acids is in agreement with the stronger acidity of HCl as compared to TFA (pKa = -8.0 and -0.25 in water, respectively [57]). Finally, it should be noted that, when treated with HCl, from the moment at which the demetallation is completed, $i_{corr.}$ undergoes a slight decrease (from t = 5 to 35 min., $i_{corr.}$ is reduced by 2.4%). That may be explained by a marginal detachment and deterioration of the porphyrin material as observed visually.

The kinetics of the cobalt(II) insertion in the porphine units of pH_2P-I was also investigated. Thus, the pH_2P-I modified electrode was dipped into a saturated solution of $Co(OAc)_2$ in DMF, under argon, at 80 °C or 110 °C, without stirring. After a given immersion time in the reactive solution, the modified electrode was rinsed with DMF and then AN and the pH_2P-I CV peak intensity at −1.2 V was assessed (Fig. 6).

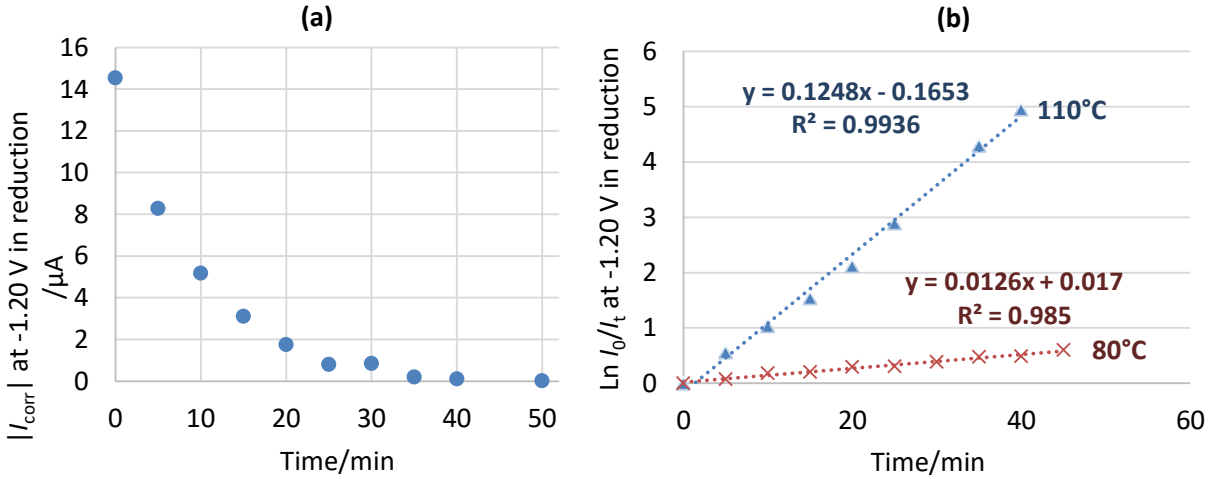

Fig. 6. (a) Evolution of pH_2P CV peak corrected intensity (absolute value) at -1.2 V as a function of time, during cobalt insertion (pH_2P modified electrode dipped in a saturated $Co(OAc)_2$ solution in DMF at 110 °C under Ar). (b) Evolution of Ln (I_0/I_t) as a function of time at 80 °C and 110 °C. I_0 is the initial intensity measured at -1.2 V (before remetallation) and I_t corresponds to the intensity measured at the same potential after *t* min of reaction in the metalating mixture (saturated $Co(OAc)_2$ solution in DMF).

Fig. 6 (a) shows the evolution of the characteristic pH_2P-I CV peak corrected intensity at -1.2 V with time, during the cobalt(II) remetallation process at 110 °C. The corrected intensity i_t was calculated by subtraction of final intensity (at 50 min.) to the measured intensity at t time. The initial peak intensity decreases and reaches a plateau after *ca*. 25 min. of reaction so that the cobalt(II) remetallation process seems to be completed at this stage. Fig. 6 (b) presents the evolution of $\ln(i_0/i_t)$ as a function of time at 110 °C and 80 °C. The linearity of the two plots (r^2= 0.993 and r^2= 0.985 for 110 °C and 80 °C, respectively) demonstrates that the remetallation reaction is a 1st order reaction *vs.* free base porphine units in the polymer. This result is consistent with previous solute porphyrin remetallation studies [35-37]. Thus, the limitation of the reaction rate does not depend from the cobalt (II) diffusion in the film but it is due to the intrinsic reactivity of the free base porphine units. Moreover the reaction rate at 110 °C is nearly ten times higher than the one calculated at 80 °C (0.125 min^{-1} and 0.0126 min^{-1} respectively), in a range of variation which is expected for a rate limiting chemical transformation.

Following these kinetic studies, for any synthesis of pCo-I, the optimized conditions indicated below were employed. pMgP-I material was demetallated with HCl for 5 min. whereas pH_2P-I modified electrode was soaked in a saturated solution of $Co(OAc)_2$ in DMF at 110 °C under Ar for 30 min.

3.3. IR-ATR Spectroscopic studies

After careful rinsing and drying under an Ar stream of pMgP-I, pH_2P-I and pCoP-I materials synthesized on a Pt disk electrode following the optimized conditions described above, e*x situ* IR-ATR measurements were performed (Fig. 7).

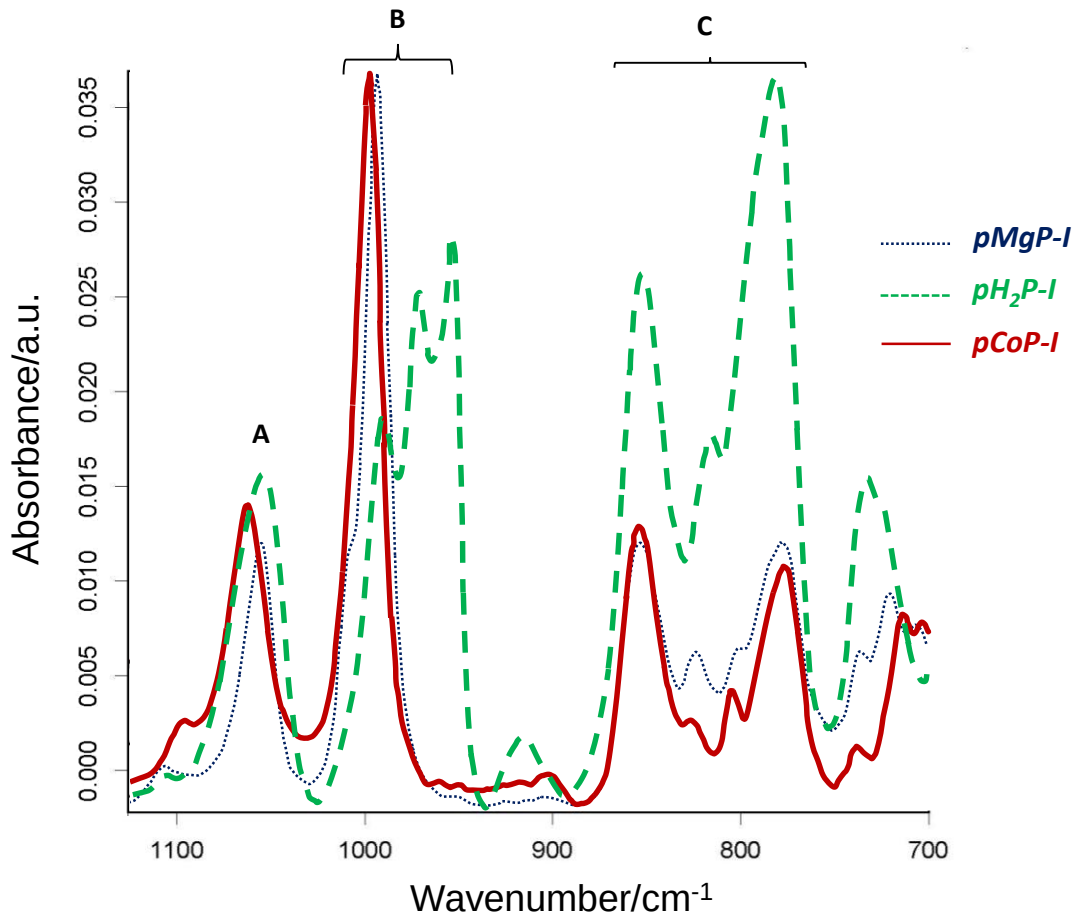

Fig. 7. IR-ATR spectra of **pMgP-I** (blue solid line), **pH$_2$P-I** (green dotted line) and **pCoP-I** (red solid line) films on Pt disk electrode.

According to previous theoretical studies from our group [21] and from other groups [58-59], vibrational bands around 1062 cm^{-1} (A) and 852 cm^{-1} (C) correspond to the different symmetry vibrations of peripheral hydrogen atoms in the porphine plane (A) and out of it (C) while vibrational amplitudes of atoms of the carbon-nitrogen skeleton are small for both bands A and C. Therefore, the demetallation/remetallation process should not radically modify the shape of the spectrum around these bands for the series pMgP-I, pH$_2$P-I and pCoP-I. This is experimentally verified with the spectra superimposed on Fig. 7 for which both the position and multiplicity of bands A and C are practically unchanged. Besides, the intense band around 990 cm^{-1} (B) is related to in-plane deformational vibrations of porphine macrocycles, with most intensive displacement of nitrogen atoms and opposite carbon atoms of NC$_4$ pyrrole rings while the central metallic cation (Mg(II) or Co(II)) remains immobile. Demetallation of porphine units leads to the violation of the forth-order symmetry of porphine and consequently to the replacement of the single intensive band by a set of much weaker ones (Fig. 7) [21]. These features proves that the Mg(II) cations are efficiently removed from the porphine macrocycles inside the polymer. After the Co(II) remetallation step is completed, the forth order symmetry must be restored. The presence of only one band at 997 cm^{-1} confirms this prediction and supports that cobalt(II) cations are efficiently inserted in the porphine ligands. Finally, these vibrational spectra afford additional evidence in favor of the conservation of the molecular structure for the three different polymers.

3.4. UV-visible measurements

Further information on the evolution of polyporphine properties was given by UV-visible absorption measurements of the different polymers (Fig. 8). For this purpose, pMgP-I was electrodeposited on an ITO plate using the optimized and already published method.[22] Then, pMgP-I was demetallated to pH_2P-I which was then remetallated with Co(II). After careful rinsing and drying under an Ar stream, UV-visible absorption spectra of pMgP-I, pH_2P-I and pCoP-I materials were recorded (Fig. 8).

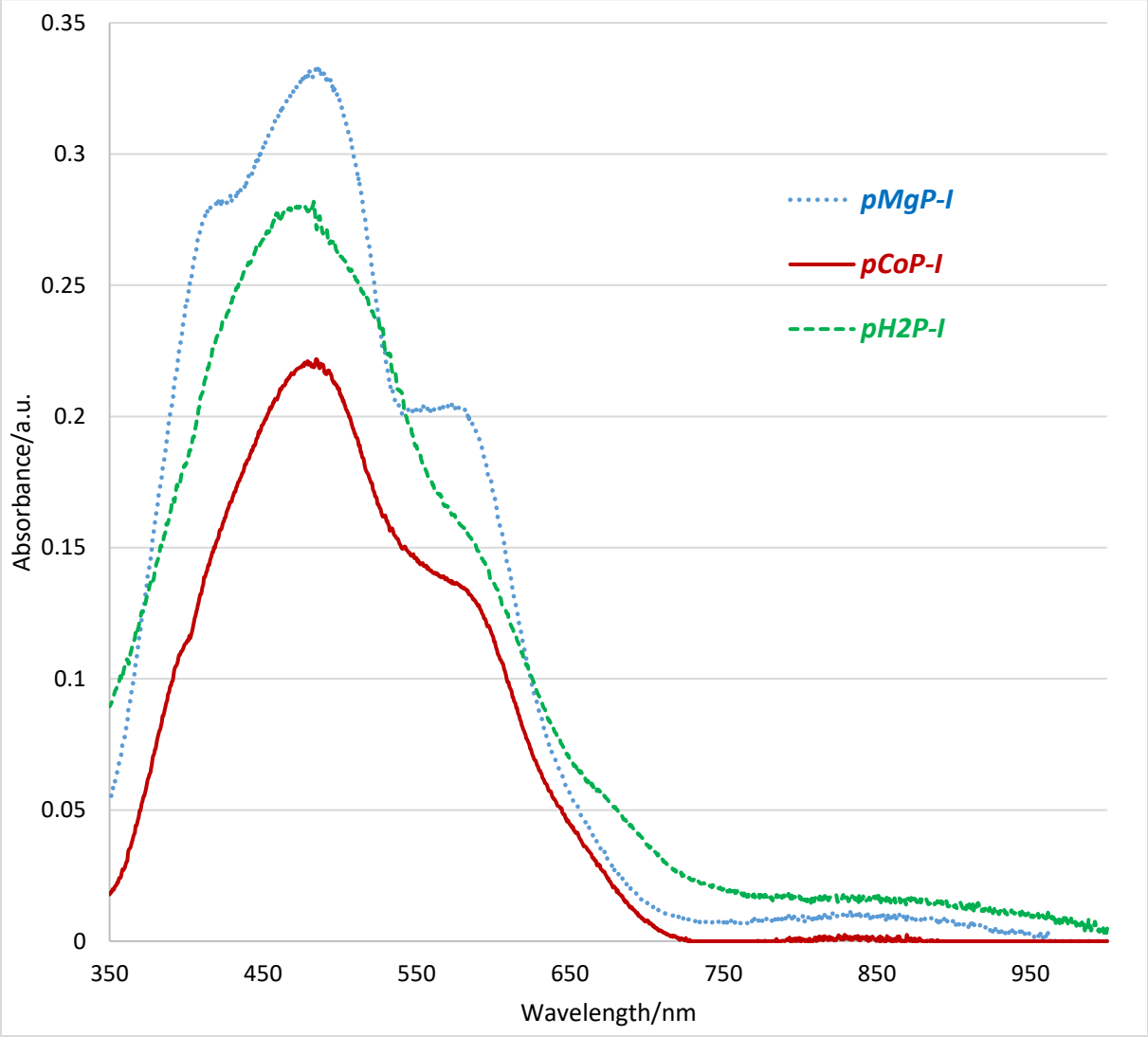

Fig. 8. UV-visible absorption spectra of **pMgP-I** (blue dotted line), **pH_2P-I** (green dashed line) and **pCoP-I** (red solid line) on ITO surface.

These UV-visible absorption spectra are very similar to those obtained for previous polyporphine materials [18,21-22] Strong broadening of the Soret and the Q bands is observed between *ca*. 400 and 500 nm and between 550 and 700 nm, respectively, for both metallated pMgP-I and pCoP-I films. The significant absorbance intensity decrease observed for pCoP-I as compared to pMgP-I is probably due to the loss of polyporphine polymer during the different steps. Thus, this decrease could stem from a weaker adhesion of polyporphine polymers on ITO plate as compared to Pt and GC substrates. The UV-visible absorption spectrum of pCoP-I resembles the pMgP-I one, in agreement with a conservation of the molecular structure and the forth order symmetry.

3.5. XPS

XPS data for various polyporphine films of type I, pMP-I, given in Fig. 9 and Table 2 lead to the conclusion that the demetallation procedure results in practically complete removal of Mg cations from the film, with its substitution with two protons per each monomer unit of the polymer. This conclusion is based on both disappearance of the Mg peak in spectrum 2 after transformation of the Mg polymer into the metal-free one (Fig. 9 left) and the modification of the N 1s peak shape (Fig. 9 right) towards a spectrum corresponding to two forms of nitrogen (amine and imine ones) inside a heterocycle [60] [61]. Subsequent replacement of these protons by Co ions (spectrum 3) is reflected by a characteristic Co peak as well as by restoration of the equivalency of all 4 nitrogen atoms. Besides, the content of oxygen increases in spectrum 3. This effect is expectedly related to a higher ability of Co ions towards axial coordination of oxygen-containing species [62] (water and atmospheric oxygen, which are due to the sample transfer via air). Similar results are obtained on glassy carbon electrodes.

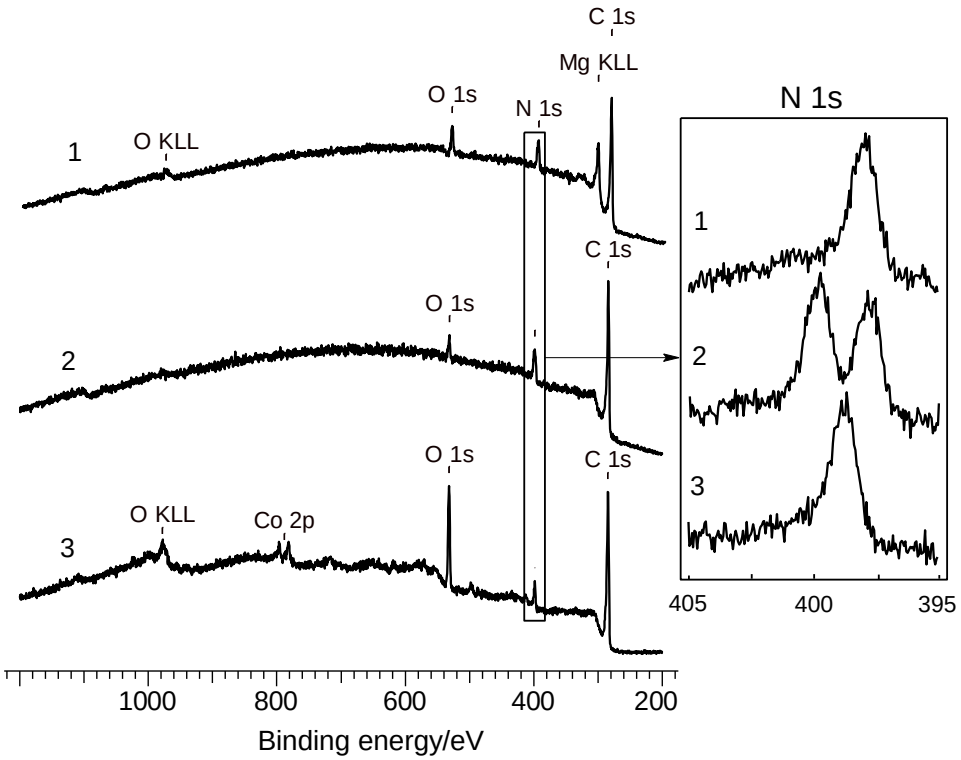

Fig. 9**.** XPS spectra of polyporphine films of type I: **pMP-I** where M = Mg (1), 2H (2) or Co (3).

On glassy carbon, the atomic ratio of C, N, Mg and Co has been calculated using peaks area of the different elements for each polymers films (Table 2). These results are in in very good agreement with an exhaustive demetalation of **pMgP-I** followed by a full cobalt(II) remetalation of **pH$_2$P-I** leading to **pCoP-I**.

Table 2. Theoretical and XPS measured atomic ratio of the **pMgP-I**, **pH$_2$P-I** and **pCoP-I**.

Polymer molecular formula (without H)	Element	Theoretical atomic ratio	Measured atomic ratio
pMgP-I **$C_{20}N_4Mg$**	**C**	20	19.7 ± 0.7
	N	4	4.0 (reference)
	Mg	1	1.0 ± 0.1
pH$_2$P-I	**C**	20	20.8 ± 0.8

$C_{20}N_4$	**N**	4	4.0 (reference)
	Mg	0	< 0.1
pCoP-I $C_{20}N_4Co$	**C**	20	20.9 ± 0.8
	N	4	4.0 (reference)
	Mg	0	< 0.1
	Co	1	1.0 ± 0.1

3.6. SEM-EDX

CV data (Figs. 2 and 3) testify in favor of a good contact of the films with substrate while no degradation is caused by their chemical or electrochemical treatment. SEM images of these films have been recorded for a more detailed study of their morphology, including the conservation of their integrity.

Images in Fig. 10 show that the surface of a film represent a flat and uniform layer composed by polymer particles of such small sizes (below 80 nm) that they are not distinguishable in these images. Aggregates of a greater-size irregular-shape particles (light objects in the images, up to 400 nm in diameter) are visible on the top of this flat layer, this location of these particles being confirmed by inclined imaging (Fig. 10 a). Local EDX spectra demonstrate that both the uniform layer and outside particles are having almost identical chemical compositions which match well to that of the polymer. Signals of P and F elements which might originate from PF_6^- containing background electrolyte are absent.

We believe that the uniform layer is composed by polymer particles growing at the film/solution interface or near it. Appearance of greater-size particles on the surface of the uniform layer is related to deposition of greater-size particles which have been formed within the diffusion layer owing to dissolved oligomers that had moved away from the surface because of a relatively low rate of the chain-growth reactions. The low rate of this reaction is due to the relative high stability of the Mg porphine cation radicals which are intermediates in the electropolymerization process. In contrast, the intermediate cation radicals involved in the formation of conventional conjugated polymers (polypyrrole, polyaniline, polythiophene) are much more reactive since the unpaired electron is less delocalized (π system less extended given the limited size of these molecules).

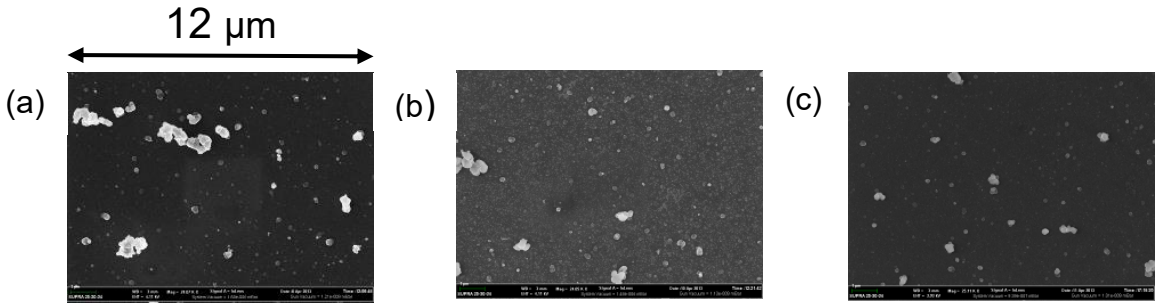

Fig. 10. SEM images of polyporphine films of type I: pMgP-I (a), pH_2P-I (b) and pCoP-I (c), on Pt substrate.

Morphologies of all these polyporphine films in Fig. 10 are similar to each other. It implies that no significant structural changes take place in the course of the central ion replacements. This observation is in agreement with CV data for these polymers on conservation of the overall intensity of the redox response. Thus, one may conclude that the used procedures retain the integrity of the film.

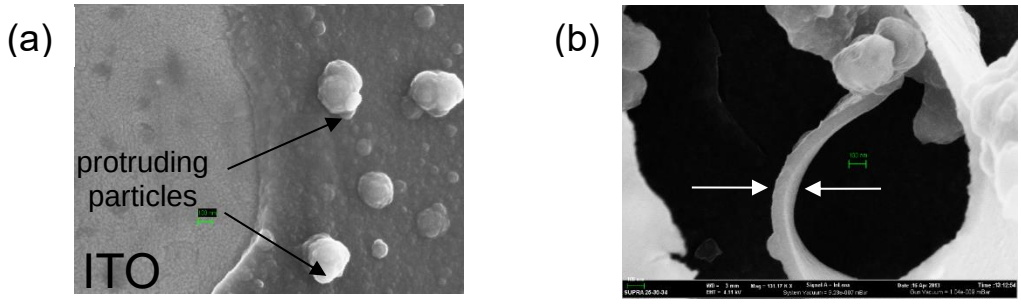

Fig. 11. SEM images of Mg polyporpine films of type I, pMgP-I, on ITO-glass surface: (a) image of the surface area (in the left part of the image) where the film was partially detached from the substrate surface so that the substrate surface is visible; (b) cross-section of the detached film (shown by arrows) used for determination of the film thickness.

SEM image of the partially detached film (Fig. 11, right image) was used to measure the thickness of this film, then to calculate the ratio of the film thickness to the deposition charge (under assumption on proportionality of these parameters of the film):

$$k = \frac{LS}{Q_{dep}} = 9.65 \pm 1.4\ nm \cdot cm^2/mC$$

where L is film thickness, S, its geometrical surface area, Q_{dep}, deposition charge.

4. Conclusion

This paper reports an easy, efficient and repeatable way to prepare the unprecedented Co(II) type I polyporphine material, pCoP-I. This material is synthesized in three steps (electrosynthesis of pMgP-I, demetallation, remetallation with Co(II)) starting from magnesium(II) porphine monomer, MgP. Optimized conditions for the demetallation and remetallation steps were found thanks to kinetics studies. The use of HCl as strong acid for the demetallation step as well as high temperature for the remetallation step were found to be key parameters for an efficient synthesis of pCoP-I. Besides, the three step formation of pCoP-I lasts less than one hour.

The electrochemical (non-electroactive interval and prepeaks conservation) and spectroscopic (similar Soret and Q bands seen on the UV-visible absorption spectra; typical porphine skeleton vibration conservation in IR-ATR) analyses demonstrate that this three step process does not alter the initial molecular structure of pMgP-I [18-20,22].

Moreover, the appearance of typical cobalt redox systems on the cyclic voltammogram (Co(III)/Co(II) and Co(II)/Co(I), see Fig. 2) as well as the recovery of the forth-order symmetry observed by IR-ATR spectroscopy after the remetallation step attest that cobalt(II) cations are inserted in the porphine macrocycles and are not simply dispersed in the material.

The final cobalt(II) type I polyporphine material could possibly be oxidized at higher potential to form type II polymer as already reported for pMgP-I, pH_2P-I and pZnP-I polymers [19,21].

Very interesting performances for the detection and the quantification of electrochemically active molecules or for relevant electrocatalytical reactions are expected thanks to the high spatial density of the active Co(II) centers in pCoP-I film. These further applicative developments are currently under investigation.

5. Acknowledgement

Financial supports from CNRS, University of Burgundy, Conseil Régional de Bourgogne (PhD grant JCE for S. Rolle), European Union and Conseil Régional de Bourgogne FABER programs are acknowledged (S.D.R., C.H.D., D.L., C.S., F.H., O.H.). C.H.D. thanks the CNRS for granting him the opportunity to work as a full time researcher for one year ("délégation CNRS", Sept. 2015). C. H. D., D. L. and S. D. R. are grateful to FILAB company, especially its Scientific Director J. Goux, for their interest in this research. Synthesis and characterization of various polyporphine films on Pt electrode by cyclic voltammetry, in situ conductivity, XPS and SEM-EDX methods (D.V.K., K.V.L., M.A.V.) were performed owing to financial support of the Russian Science Foundation (grant 14-13-01244).

6. References

[1] S. Griveau and F. Bedioui, in: K.M. Kadish, K.M. Smith and R. Guilard (Ed.), Handbook of Porphyrin Science ith Application to Chemistry, Physics, Materials Science, Engineering, Biology and Medecine. , vol. 12, World Scientific, 2011, 227-295.
[2] A. Wang, Y. Fang, L. Long, Y. Song, W. Yu, W. Zhao, M.P. Cifuentes, M.G. Humphrey and C. Zhang, Facile Synthesis and Enhanced Nonlinear Optical Properties of Porphyrin-Functionalized Multi-Walled Carbon Nanotubes, Chemistry – A European Journal 19 (2013) 14159-14170.
[3] R.F. Khairutdinov and N. Serpone, Photoluminescence and Transient Spectroscopy of Free Base Porphyrin Aggregates, The Journal of Physical Chemistry B 103 (1999) 761-769.
[4] S.H. Kazemi, B. Hosseinzadeh and S. Zakavi, Electrochemical fabrication of conducting polymer of Ni-porphyrin as nano-structured electrocatalyst for hydrazine oxidation, Sensors and Actuators B: Chemical 210 (2015) 343-348.
[5] S. Ishihara, J. Labuta, W. Van Rossom, D. Ishikawa, K. Minami, J.P. Hill and K. Ariga, Porphyrin-based sensor nanoarchitectonics in diverse physical detection modes, Physical Chemistry Chemical Physics 16 (2014) 9713-9746.
[6] Y.-L.C. Shen-Ming Chen, R. Thangamuthu, Electropolymerization of iron tetra(o-aminophenyl) porphyrin from aqueous solution and the electrocatalytic behavior of modified electrode, Journal of Solid State Electrochemistry 11 (2007) 1441-1448.
[7] A.U. Alberto Gómez-Caballero, Alicia Sánchez-Ortega, Nora Unceta, M. Aranzazu Goicolea, Ramón J. Barrio Molecularly imprinted poly[tetra(o-aminophenyl)porphyrin] as a stable and selective coating for the development of voltammetric sensors, J. Electroanal. Chem. 638 (2010) 246-253.
[8] E. Mazzotta and C. Malitesta, Electrochemical detection of the toxic organohalide 2,4-DB using a Co-porphyrin based electrosynthesized molecularly imprinted polymer, Sensors and Actuators B: Chemical 148 (2010) 186-194.
[9] A.C. Paske, L.D. Earl and J.L. O'Donnell, Interfacially polymerized metalloporphyrin thin films for colorimetric sensing of organic vapors, Sensors and Actuators B: Chemical 155 (2011) 687-691.
[10] M.D.P.T.S. Ademar Wong, Biomimetic sensor based on 5,10,15,20-tetrakis(pentafluorophenyl)-21H,23H-porphyrin iron (III) chloride and MWCNT for selective detection of 2,4-D, Sensors and Actuators B 181 (2013) 332-339.
[11] L. Lvova, C. Di Natale and R. Paolesse, Porphyrin-based chemical sensors and multisensor arrays operating in the liquid phase, Sensors and Actuators B: Chemical 179 (2013) 21-31.
[12] C.-W. Kung, T.-H. Chang, L.-Y. Chou, J.T. Hupp, O.K. Farha and K.-C. Ho, Porphyrin-based metal–organic framework thin films for electrochemical nitrite detection, Electrochemistry Communications 58 (2015) 51-56.
[13] R.L. McCreery, Molecular Electronic Junctions, Chemistry of Materials 16 (2004) 4477-4496.
[14] A.P. Bonifas and R.L. McCreery, Assembling Molecular Electronic Junctions One Molecule at a Time, Nano Letters 11 (2011) 4725-4729.
[15] S. Trevin, F. Bedioui, M. Guadalupe Gomez Villegas and C. Bied-Charreton, Electropolymerized nickel macrocyclic complex-based films: design and electrocatalytic application, J. Mater. Chem. 7 (1997) 923-928.
[16] T. Malinski and Z. Taha, Nitric oxide release from a single cell measured in si tu by a porphyrinic-based microsensor, Nature 358 (1992) 676-678.
[17] C.H. Devillers, D. Lucas, A.K.D. Dimé, Y. Rousselin and Y. Mugnier, Exploring the redox reactivity of magnesium porphine. Insight into the origins of electropolymerisation, Dalton Trans. 39 (2010) 2404–2411.
[18] M.A. Vorotyntsev, D.V. Konev, C.H. Devillers, I. Bezverkhyy and O. Heintz, Magnesium(II) polyporphine: The first electron-conducting polymer with directly linked unsubstituted porphyrin units obtained by electrooxidation at a very low potential, Electrochimica Acta 55 (2010) 6703-6714.
[19] M.A. Vorotyntsev, V.K. Dmitry, C.H. Devillers, I. Bezverkhyy and O. Heintz, Electroactive polymeric material with condensed structure on the basis of magnesium(II) polyporphine, Electrochimica Acta 56 (2011) 3436–3442.

[20] D.V. Konev, M.A. Vorotyntsev, C.H. Devillers, T.S. Zyubina, A.S. Zyubin, K.V. Lizgina and A.G. Volkov, Synthesis of new polyporphines by replacing central ion in magnesium polyporphine, Russ. J. Electrochem. 49 (2013) 753-758.
[21] D.V. Konev, C.H. Devillers, K.V. Lizgina, T.S. Zyubina, A.S. Zyubin, L.A. Maiorova- Valkova and M.A. Vorotyntsev, Synthesis of new electroactive polymers by ion-exchange replacement of Mg(II) by 2H+ or Zn(II) cations inside Mg(II) polyporphine film, with their subsequent electrochemical transformation to condensed-structure materials, Electrochimica Acta 122 (2014) 3-10.
[22] D.V. Konev, C.H. Devillers, K.V. Lizgina, V.E. Baulin and M.A. Vorotyntsev, Electropolymerization of non-substituted Mg(II) porphine: Effects of proton acceptor addition, J. Electroanal. Chem. 737 (2015) 235-242.
[23] C.A. Xavi Cetó, Manel del Valle, Maria Luz Rodríguez-Méndez Evaluation of red wines antioxidant capacity by means of a voltammetric e-tongue with an optimized sensor array, Electrochimica Acta 120 (2014) 180-186.
[24] H. Gu, X. Huang, L. Yao, E. Teye and Y. Wen, Study on the binding ability of cobalt-porphyrin with small volatile organic compounds based on density functional theory, Analytical Methods 6 (2014) 3360-3364.
[25] K.I. Ozoemena, Z. Zhao and T. Nyokong, Immobilized cobalt(II) phthalocyanine–cobalt(II) porphyrin pentamer at a glassy carbon electrode: Applications to efficient amperometric sensing of hydrogen peroxide in neutral and basic media, Electrochemistry Communications 7 (2005) 679-684.
[26] J.H. Vélez, J.P. Muena, M.J. Aguirre, G. Ramirez and F. Herrera, Electrchemical Oxidation of Sulfite in Aqueous Solution byGlassy Carbon Electrode Modified ith Polymeric Co(II) Meso-Tetrakis (2-Thienyl)Porphyrin, International Journal of ELECTROCHEMICAL SCIENCE 7 (2012) 3167-3177.
[27] C.A. Pessôa and Y. Gushikem, Cobalt porphyrins immobilized on niobium(V) oxide grafted on a silica gel surface: study of the catalytic reduction of dissolved dioxygen, Journal of Porphyrins and Phthalocyanines 05 (2001) 537-544.
[28] V.A. Bogdanovskaya, L.A. Beketaeva, K.V. Rybalka, B.N. Efremov, N.M. Zagudaeva, M. Sakashita, T. Iidzima and Z.R. Ismagilov, Nanosize catalysts based on carbon materials promoted by cobalt tetra(para-methoxyphenyl) porphyrin pyropolymer for oxygen electroreduction, Russ. J. Electrochem. 44 (2008) 293-302.
[29] T.D. Chung and F.C. Anson, Catalysis of the electroreduction of O2 by cobalt 5,10,15,20-tetraphenylporphyrin dissolved in thin layers of benzonitrile on graphite electrodes, J. Electroanal. Chem. 508 (2001) 115-122.
[30] C. Shi and F.C. Anson, Catalysis of the Electro-Oxidation of Carbon Monoxide by Cobalt Octaethylporphyrin, Inorganic Chemistry 40 (2001) 5829-5833.
[31] D.K. Dogutan, M. Ptaszek and J.S. Lindsey, Direct Synthesis of Magnesium Porphine via 1-Formyldipyrromethane, The Journal of Organic Chemistry 72 (2007) 5008-5011.
[32] C.H. Devillers, A.K.D. Dimé, H. Cattey and D. Lucas, Crystallographic, spectroscopic and electrochemical characterization of pyridine adducts of magnesium(II) and zinc(II) porphine complexes, Comptes Rendus Chimie 16 (2013) 540-549.
[33] C. Inisan, J.-Y. Saillard, R. Guilard, A. Tabard and Y. Le Mest, Electrooxidation of porphyrin free bases: fate of the [small pi]-cation radical, New Journal of Chemistry 22 (1998) 823-830.
[34] C.H. Devillers, A. Milet, J.-C. Moutet, J. Pecaut, G. Royal, E. Saint-Aman and C. Bucher, Long-range electronic connection in picket-fence like ferrocene-porphyrin derivatives, Dalton Transactions 42 (2013) 1196-1209.
[35] L.R. Robinson and P. Hambright, The kinetics of zinc(II) incorporation into fifty-five free base porphyrins in DMF: structure-reactivity correlations, Inorganica Chimica Acta 185 (1991) 17-24.
[36] H. Peter, Aspects of metal ion incorporation into porphyrin molecules, Annals New York Academy of Sciences (1973) 443-452.
[37] F.R. Longo, E.M. Brown, D.J. Quimby, A.D. Adler and M. Meot-Ner, Kinetic studies on metal chelation by porphyrins, Annals of the New York Academy of Sciences 206 (1973) 420-442.
[38] P. Worthington, P. Hambright, R.F.X. Williams, J. Reid, C. Burnham, A. Shamim, J. Turay, D.M. Bell, R. Kirkland, R.G. Little, N. Datta-Gupta and U. Eisner, Reduction potentials of seventy-five free

base porphyrin molecules: Reactivity correlations and the prediction of potentials, Journal of Inorganic Biochemistry 12 (1980) 281-291.
[39] P. Worthington, P. Hambright, R.F.X. Williams, M.R. Feldman, K.M. Smith and K.C. Langry, Reduction potentials of beta-substituted free base porphyrins, Inorganic and Nuclear Chemistry Letters 16 (1980) 441-447.
[40] J.-H. Fuhrhop, in: K.M. Smith (Ed.), Porphyrins and Metalloporphyrins, vol. Elsevier Scientific Publishing Compagny, 1975, 601.
[41] C. Shi, B. Steiger, M. Yuasa and F.C. Anson, Electroreduction of O2 to H2O at Unusually Positive Potentials Catalyzed by the Simplest of the Cobalt Porphyrins, Inorganic Chemistry 36 (1997) 4294-4295.
[42] K.M. Kadish, E.V. Caemelbecke and G. Royal, in: K.M. Kadish, K.M. Smith and R. Guilard (Ed.), The Porphyrin Handbook vol. 8, 2000, 61-69.
[43] J.P.M. J.H. Vélez, M.J. Aguirre, G. Ramirez, Francisco Herrera, Electrochemical Oxidation of Sulfite in Aqueous Solution by Glassy Carbon Electrode Modified with Polymeric Co(II) Meso-Tetrakis(2-Thienyl)Porphyrin, Int. J. Electrochem. Sci. 7 (2012) 3167-3177.
[44] S. Cosnier, A. Deronzier and J.F. Roland, Polypyridinyl complexes of ruthenium(II) having 4,4'-dicarboxy ester-2,2'-bipyridine ligands attached covalently to polypyrrole films: Reinvestigation of the polypyrrole electrochemical response in poly[tris(N-bipyridylethyl)pyrrole] ruthenium(II) films, J. Electroanal. Chem. 285 (1990) 133-147.
[45] S. Cosnier, C. Gondran, K. Gorgy, R. Wessel, F.-P. Montforts and M. Wedel, Electrogeneration and characterization of a poly(pyrrole–nickel (II) chlorin) electrode, Electrochemistry Communications 4 (2002) 426-430.
[46] S. Cosnier, C. Gondran, R. Wessel, F.-P. Montforts and M. Wedel, Poly(pyrrole–metallodeuteroporphyrin)electrodes: towards electrochemical biomimetic devices, J. Electroanal. Chem. 488 (2000) 83-91.
[47] J. Yang, Y. Yang, J. Hou, X. Zhang, W. Zhu, M. Xu and M. Wan, Polypyrrole—polypropylene composite films: preparation and properties, Polymer 37 (1996) 793-798.
[48] S. Gottesfeld, A. Redondo, I. Rubinstein and S.W. Feldberg, Resistance-induced peaks in cyclic voltammograms of systems that can be switched electrochemically between an insulating and conductive state, J. Electroanal. Chem. 265 (1989) 15-22.
[49] M.A. Vorotyntsev, M. Skompska, E. Pousson, J. Goux and C. Moise, Memory Effects in Functionalized Conducting Polymer Films: Titanocene Derivatized Polypyrrole in Contact with THF Solutions, J. Electroanal. Chem. 552C (2003) 307-317.
[50] M. Feinberg, Validation interne des methodes d'analyses, Techniques de l'ingénieur (2001)
[51] Accuracy (trueness and precision) of measurement methods and results - Part 1: General principles and definitions, ISO 5725-1 (1994)
[52] M.A. Vorotyntsev and D.V. Konev, Primary and Secondary Distributions after a Small-Amplitude Potential Step at Disk Electrode Coated with Conducting Film, Electrochim. Acta 56 (2011) 9105–9112.
[53] J. Li, J.R. Diers, J. Seth, S.I. Yang, D.F. Bocian, D. Holten and J.S. Lindsey, Synthesis and Properties of Star-Shaped Multiporphyrin−Phthalocyanine Light-Harvesting Arrays, The Journal of Organic Chemistry 64 (1999) 9090-9100.
[54] B. Don and T.F. Yen, in: (Ed.), Catalysis and Reaction Kinetics Role Trace Met. Pet., vol. Ann Arbor Sci., Ann Arbor, Mich, Univ. South. California Los Angeles, CA, USA 1975, 195-200.
[55] B. Pazv, C. Yo-Ying, R. Galo, J.C. Maria, M. Betty, Leonora Mendoza, Mauricio Isaacs, Macarena García, M.C. Arevalo and M.J. Aguirre, Electrooxidation and determination of sulfite in ethanol–water solutions using poly-Cu(II)-tetrakis(x-aminophenyl)porphyrin/glassy carbon modified electrodes, Collect. Czech. Chem. Commun. 74 (2009) 545-557.
[56] W.L. Reynolds, K. Kooda, B. Florine, N. Johnson and K. Thielman, Demetallation of α,β,γ,δ-tetrakis(p-sulfophenyl) porphiniron(III) in mineral acid–alcohol–water media, International Journal of Chemical Kinetics 12 (1980) 97-105.

[57] F.G. Bordwell, Equilibrium acidities in dimethyl sulfoxide solution, Acc. Chem. Res. 21 (1988) 456-463.
[58] Z. Zhang, A.L. Verma, M. Yoneyama, K. Nakashima, K. Iriyama and Y. Ozaki, Molecular Orientation and Aggregation in Langmuir−Blodgett Films of 5-(4-N-Octadecylpyridyl)-10,15,20-tri-p-tolylporphyrin Studied by Ultraviolet−Visible and Infrared Spectroscopies, Langmuir 13 (1997) 4422-4427.
[59] N.V. Ivashin, Calculation of the structure and vibrational states for anionic forms of Co-, Ni-, and Cu-porphines, J Appl Spectrosc 77 (2010) 28-37.
[60] S.A. Krasnikov, N.N. Sergeeva, M.M. Brzhezinskaya, A.B. Preobrajenski, Y.N. Sergeeva, N.A. Vinogradov, A.A. Cafolla, M.O. Senge and A.S. Vinogradov, An x-ray absorption and photoemission study of the electronic structure of Ni porphyrins and Ni N-confused porphyrin, Journal of Physics: Condensed Matter 20 (2008) 235207.
[61] C. Wang, Q. Fan, S. Hu, H. Ju, X. Feng, Y. Han, H. Pan, J. Zhu and J.M. Gottfried, Coordination reaction between tetraphenylporphyrin and nickel on a TiO2(110) surface, Chemical Communications 50 (2014) 8291-8294.
[62] I. Hatay, B. Su, F. Li, M.A. Méndez, T. Khoury, C.P. Gros, J.-M. Barbe, M. Ersoz, Z. Samec and H.H. Girault, Proton-Coupled Oxygen Reduction at Liquid−Liquid Interfaces Catalyzed by Cobalt Porphine, J. Am. Chem. Soc. 131 (2009) 13453-13459.